3D photoionization structure and distances of Planetary Nebulae III. NGC 6781[1]

Hugo E. Schwarz[1], Hektor Monteiro[2]
[1]Cerro Tololo Inter-American Observatory, Casilla 603, Colina El Pino s/n, La Serena [Chile]
[2]Department of Physics and Astronomy, Georgia State University, Park Place South, Atlanta, GA 30302 [United States of America]
Nucleo de Astrofisica-CETEC- Unicsul .
hschwarz@ctio.noao.edu

Continuing our series of papers on the three-dimensional (3D) structures and accurate distances to Planetary Nebulae (PNe), we present our study of the planetary nebula NGC6781. For this object we construct a 3D photoionization model and, using the constraints provided by observational data from the literature we determine the detailed 3D structure of the nebula, the physical parameters of the ionizing source and the first precise distance. The procedure consists in simultaneously fitting all the observed emission line morphologies, integrated intensities and the two-dimensional (2D) density map from the [SII] (sulfur II) line ratios to the parameters generated by the model, and in an iterative way obtain the best fit for the central star parameters and the distance to NGC6781, obtaining values of 950±143 pc (parsec – astronomic distance unit) and 385 $L^{\odot}$ (solar luminosity) for the distance and luminosity of the central star respectively. Using theoretical evolutionary tracks of intermediate and low mass stars, we derive the mass of the central star of NGC6781 and its progenitor to be 0.60±0.03$M^{\odot}$ (solar mass) and 1.5±0.5$M^{\odot}$ respectively.

Key words: Interstellar medium. Photoionization modeling. Planetary Nebula.

1 Introduction

Planetary Nebulae (PNe) are the end products of the evolution of stars with masses below about 8M$_\odot$ (POTTASCH, 1984; IBEN JUNIOR; RENZINI, 1983). The importance of these objects extends beyond the understanding of how the outer layers of stars end up forming the many observed morphologies. Indeed, PNe have been used for many purposes, from understanding basic atomic and plasma processes (ALLER, 1987) to determine chemical evolution of our galaxy (IDIART; COSTA; MACIEL, 2003). Recently PNe are also being used to study galaxies other than our own, providing powerful tools to determine distances, kinematics and chemical properties of external galaxies (CIARDULLO, 2003) and even to trace inter-cluster material as in Feldmeier and collaborators (2004). PNe have the advantage that they are observable out to large distances due to their luminous narrow emission lines, especially [OIII] (oxigen III) 500.7 nanometers (nm), being useful also as standard candles through the use of the PN (Planetary Nebula) and the luminosity function (JACOBY; CIARDULLO; FELDMEIER, 1999).

One of the most important problems in observational Galactic PNe research is the difficulty in determining their distances and three-dimensional (3D) structures. Observations always produce a two-dimensional (2D) projection of their 3D structure, and recovering the original structure is not trivial. This is also made worse by the fact that only crude distances, usually obtained from statistical methods on large samples, can be determined. Large uncertainties are generated by the need to assume constancy of one parameter such as the nebular size, (ionized) mass, flux etc. so that typical errors in the distances to individual objects are of the order of a factor of three or more. Very few nebulae have had individual accurate distances determined.

Historically, PNe have been studied with empirical methods and one dimensional (1-D) photoionization models, leading to the above mentioned problems. In contrast to this, our technique developed and described in Monteiro and collaborators (2004) provides precise, self-consistently determined distances, as well as the physical parameters for the central star and gaseous nebula, for objects with sufficient observational constraints. These objects can provide valuable calibration for existing distance scales as well as self-consistently determined physical and chemical quantities. For a detailed description of our novel method see our previously published papers in this series and especially the extensive explanatory appendix in the second paper Monteiro and collaborators (2005).

In this work we focus on the PN of NGC6781 (RA 19h 18m 28s Dec. +06o 32' 19" 2000) shown in Illustration 1. This is a PN whose main structure is observed as a 130" diameter bright shell of low ellipticity, double in parts and with fainter lobes emanating at the North-South (N-S) ends where the ring is double and fainter. The ring is brighter in the East-West (E-W) directions as also shown in Illustration 1 of Mavromatakis, Papamastorakis and Paleologou (2001). Their image is available as a fits file on the web[2] and our Illustration 1 has been produced using this image.

Mavromatakis, Papamastorakis and Paleologou (2001) claim a possible faint halo extending out to about 3' by 4' surrounding NGC6781. Note that Corradi and collaborators (2003) list the object in their paper on the search for faint haloes around bright PNe, but does not make any statement about having detected a halo according to their criteria, which include the candidate halo having to be limb brightened and/or detached. The halo of Mavromatakis, Papamastorakis and Paleologou (2001) is not limb brightened and more likely to be the result of scattered light in the instrument.

For a more detailed discussion of the morphology of NGC6781 based on a set of narrow band images, as well as density, temperature, and extinction maps see Mavromatakis, Papamastorakis and Paleologou (2001).

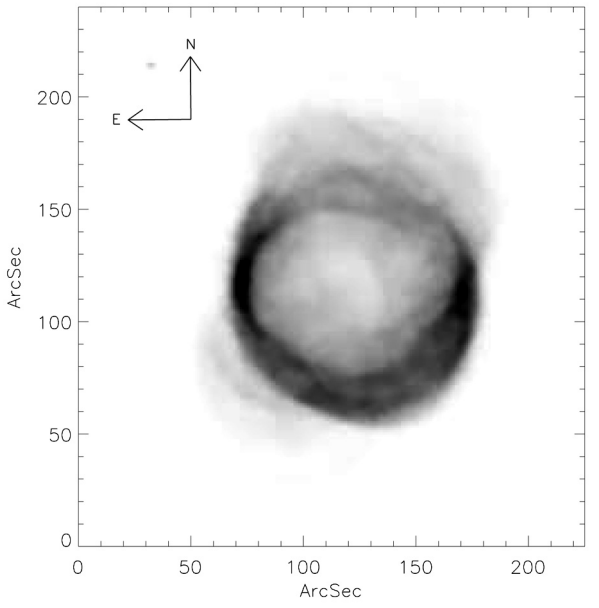

Illustration 1: Narrowband image of NGC6781 in the light of the [NII] (Nitrogen II) 658.4 nm line

Source: Mavromatakis, Papamastorakis and Paleologou (2001).

An estimate for the luminosity, temperature, and mass of the CS of NGC6781 based on statistical analysis is 127 $L^{\odot}$ (solar luminosity), 105 kK (kilo Kelvin), and 0.6$M^{\odot}$ (solar mass) respectively, taken from Stanghellini and collaborators (2002). The average distance of the 12 literature values we found in Acker and collaborators (1992) is 946 pc with the individual values ranging from 500 to 1,600 pc, a factor of more than three.

The spectral energy distribution (SED) of NGC6781 shows a broad blackbody-like spectrum between about 1 and 100 μm, a radio tail out to 12 cm, and a rise toward the blue which probably comes from the hot central star. Integrating the SED curve we obtain a luminosity of L = 166.d^2 (kpc). $L^{\odot}$ The luminosity of NGC6781

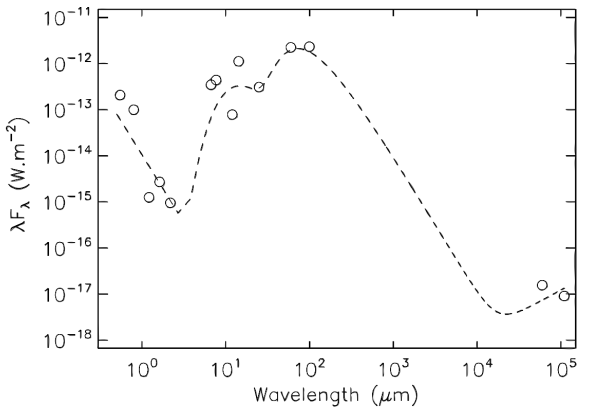

Illustration 2: The graph shows the spectral energy distribution (SED) of NGC6781 over more than five decades of wavelength interval. All values were obtained from the literature. The dotted curve is a combined blackbody and continuum radiation fit to the data

Source: The authors.

is therefore 150 $L^{\odot}$ at its distance of 950 pc. Applying the usual correction according to Myers and collaborators (1987) we obtain L = 225 $L^{\odot}$.

Here we present our own modeling results using observational data published in the literature as constraints and derive the 3D structure, chemical abundances, CS (central star) properties, and distance for NGC6781 in a self-consistent manner.

In the paragraph two, we discuss the observational data used as constraints for the models. In the paragraph three, we present the model results generated by the 3D photoionization code, and we discuss the derived quantities. In the paragraph four, we give our overall conclusions and discuss possible discrepancies with other determinations of parameters for this nebula.

2 Observations

The observational data that we used to constrain our model for NGC6781 were taken from the literature. Mavromatakis, Papamastorakis and Paleologou (2001) presents narrow band imaging

of the nebula in the most important lines such as H_α, H_θ ,[OIII] and others. He also provides [SII] narrow band images to obtain a spatially resolved density map, as well as the H_α, H_θ extinction map of the nebula. We used their 2D density map to infer the 3D density structure to be used as an input for the photoionization model.

Liu and collaborators (2004) present deep optical spectra of medium resolution for NGC 6781 and 11 other PNe. The observations were carried out with a long-slit spectrograph covering from 360 to 800 nm and include all important emission lines. Their observations are particularly interesting because the objects were scanned with the long-slit across the nebular surface by driving the telescope differentially in right ascension. These observations then yield average spectra for the whole nebula, which are in principle more precise than single slit observations, and allow us to produce emission line maps of the object. For details of the observations and their reduction procedure as well as the full tables of line fluxes, see Liu and collaborators (2004). The most important lines used as constraints for the model are listed in our Table 1 together with the corresponding values from our model.

We also used the H_α +[NII] image from Mavromatakis, Papamastorakis and Paleologou (2001) to determine the size of NGC6781 thus using it as one of the constraints for the distance obtained in our model calculations.

Table 1: Observed and model line fluxes and model central star parameters for NGC6781

	Observed	Model	Relative Error
T. (K)	–	123 kK	–
$L/L^{\odot}$	–	385	–
log (g.)	–	7.0	–
Distance (pc)	500-1600	950	±0.143
Density	100-1400	100-1400	–
He/H	–	1.25×10^{-1}	–
C/H	–	5.95×10^{-4}	–
N/H	–	9.75×10^{-5}	–
O/H	–	3.50×10^{-4}	–
Ne/H	–	7.10×10^{-5}	–
Ar/H	–	2.26×10^{-6}	–
S/H	–	0.28×10^{-5}	–
log (H_θ)	-9.80	-9.84	-0.09
[NeIII] 386.8[a]	1.09	1.06	-0.03
[OIII] 436.3	0.05	0.07	0.28
HeII 468.6	0.09	0.09	0.02
[OIII] 500.7	8.23	7.10	-0.14
[NII] 575.5	0.07	0.07	0.07
HeI 587.6	0.16	0.17	0.09
[OI] 630.2	0.33	0.38	0.15
H_θ 656.3	2.65	2.86	0.08
[NII] 658.4	3.96	3.88	-0.02
[SII] 671.7	0.25	0.25	-0.01
[SII] 673.1	0.21	0.21	0.00

Source: Kaler, Shaw and Browning (1997).

3 Photoionization models for NGC6781

The photoionization code we used for the study of NGC6781 is the Mocassin code described in full detail in Ercolano and collaborators (2003). This code allows for the same possibilities as the code used previously in Monteiro and collaborators (2000) but is more sophisticated in that the diffuse radiation is fully taken into account in an efficient manner. The previous code also had this ability but the associated increase in computational time was prohibitive.

The basic procedure adopted to study NGC6781 is the same, independent of the code and has been fully described in the two previous papers in this series (MONTEIRO et al., 2004; 2005). In short, we gather as much observational material as possible and use it to constrain our model with many data simultaneously. Of particular interest are the total line fluxes and line images corrected for reddening, and the line diagnostic ratio maps. The structure adopted for the nebu-

lae is defined based on the observed density map, when available, or density profiles from single slit observations plus the observed projected morphology in several emission lines.

In the case of NGC6781 in particular, the initial structure was based on density maps published by Mavromatakis, Papamastorakis and Paleologou (2001). It is clear from the images and density map (from the [SII] (sulfur II) doublet ratio) presented here, that the density is lower in the central region than in the main bright ring. This indicates that the structure must have lower density material in the line of sight of those regions and therefore the best structure to reproduce the observed projected morphology is an open ended structure or hour-glass shape, which we therefore adopt for this object. It is also clear from the images in many narrow band filters that the material is highly clumpy, so to reproduce this we include random density fluctuations in the adopted structure. The final adopted structure in its best fitting orientation on the sky is presented in Illustration 3.

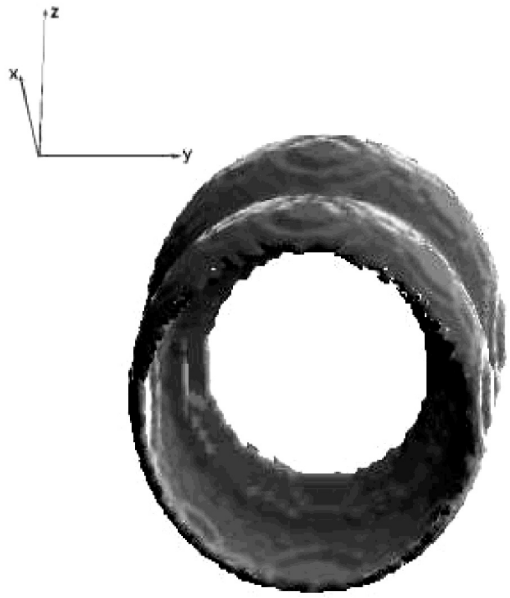

Illustration 3: The image shows an isodensity surface of the structure adopted for NGC6781 in its final fitted spatial orientation indicated in the upper left hand corner

Source: The authors.

4 Model results

We present here the main results obtained from the photoionization model constrained by the observational data. The integrated fluxes for 12 emission lines are given in Table 1, as well as the fitted abundances and ionizing star parameters.

The model fitting procedure which uses the model image size fitted to the observed one for the line [NII] 658.4 nm, as well as the absolute H_θ, flux, and the integrated fluxes of all other lines gives a distance of 950±145 pc for NGC6781. The error on this distance has been computed in the same way as in our previous papers in this series.

In Illustration 4 we show the projected images obtained from the fitted model. Notice that all major morphological features of the object are well reproduced as well as the general ionization stratification in the different emission lines. In particular the images for [OIII] 500.7 and HeII (Helium II) 468.6 show very good agreement with those obtained by Mavromatakis, Papamastorakis and Paleologou (2001) as well as the more common [NII] 658.4 nm and H_θ.

Illustration 5 shows the final model image for [NII] 658.4 nm plotted in contours over the observed image by Mavromatakis, Papamastorakis and Paleologou (2001). Again the good agreement of the apparent size, obtained from the size of the fitted model grid and our determined distance, is evident.

As with objects studied in previous works, the mass of the ionizing star, as well as its progenitor and age are determined from theoretical cooling tracks. Here we have used the cooling tracks

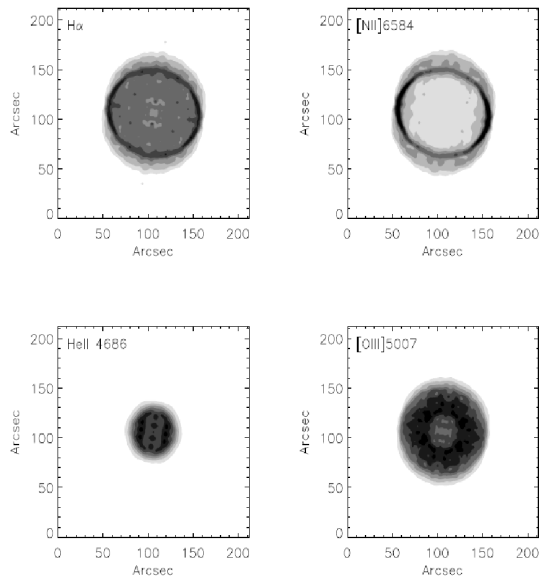

Illustration 4: Images obtained from the projection at the observed angle of the data cubes of emissivities computed by the photoionization code for the most important emission lines. Compare these model images with the observed images in Mavromatakis, Papamastorakis and Paleologou (2001)

Source: The authors.

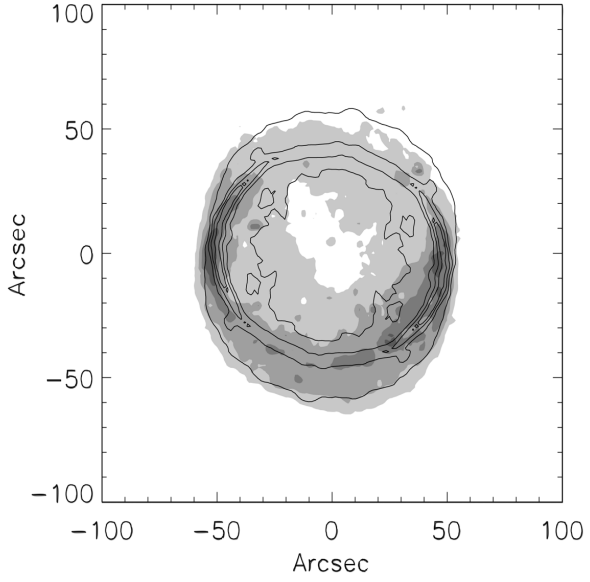

Illustration 5: Image comparing the observed [NII] 658.4 nm narrow band image with the contours of the equivalent image of the fitted model. Note the similarity between the observed and modeled images

Source: The authors.

of Vassiliadis and Wood (1994) because their grids present a good (= close) sampling of progenitor masses in the 1 to 3M$^{\Theta}$ range. In Illustration 6 we show the position of NGC6781, as well as the other objects that we have studied previously with this method, along with the theoretical cooling tracks. From this we obtain the mass of the central star of and its progenitor to be 0.60±0.03M$^{\Theta}$ and 1.5±0.5M$^{\Theta}$ respectively. Illustration 6 also shows the position of these same objects as determined by different authors by distinct techniques. All

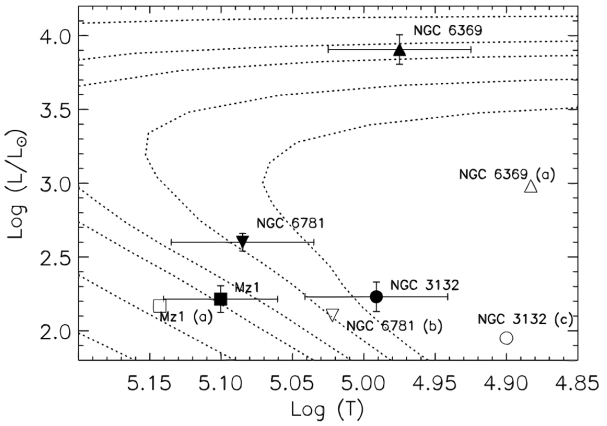

Illustration 6: HR diagram for NGC6781, NGC3132 (MONTEIRO et al., 2000), NGC6369 (MONTEIRO et al., 2004), MZ 1 (MONTEIRO et al., 2005), all PNe that had their central star properties determined by our method. Also plotted are the literature values for comparison

Obs.: a) Stanghellini, Corradi and Schwarz (1993); b) Stanghellini and collaborators (2002); c) The evolutionary tracks are from Vassiliadis and Wood (1994); they are similar to the Blocker (1995) models but take metalicities etc. into account.

Source: The authors.

PNe central stars are well evolved on their cooling track except NGC6369.

5 Discussion and conclusions

As with all our other PNe central star temperatures determined by this 3D structure method we generally find higher temperatures than those computed from oxygen lines and nearer those from HeII lines. Table 2 shows a comparison of

Table 2: Comparison of parameters found in the literature and those determined by our 3D method

Object	Our T	HeII/HI	[OIII]/ [OII]	Our L ($L^{\odot}$)	Our d (pc)
H^{b} 5	230[a]	131[b]	–	6000[a]	1400[a]
Mz1	120[c]	139[d]	–	164[c]	1050[c]
NGC 3132	90[e]	80[c]	36[c]	150[e]	930[e]
NGC 6369	91[f]	122[g]	60[g]	8100[f]	1550[f]
NGC 6781	123[h]	126[g]	68[g]	385[h]	950[h]

Obs.: a) Preliminary results from Rice, Schwarz and Monteiro (2004); b) Kaler and Jacoby (1989); c) Phillips (2003); d) Monteiro and collaborators (2005); e) Monteiro and collaborators (2000); f) Monteiro and collaborators (2004); g) Gurzadyan (1997); h) This paper.

Source: The authors.

parameters from the literature and those determined by us in this and previous papers.

Note that Phillips (2003) found that bipolar PNe have average T (HeII) = 138 Kelvin (K); ellipticals 92 k; round 81 k whole sample 87 k. This was also found earlier by Corradi and Schwarz (1995) who determined T (bipolars) = 142 k; irregulars 99 k; ellipticals 76 k; and unresolved 63 k. This general trend is always observed, and our high temperature for bipolar NGC6781 is no exception.

The central star properties of all PNe that we have applied our method are shown in the HR diagram of Illustration 6. Also shown are the values determined by other methods, taken from the literature. There are large differences between our values and those previously published for NGC6781 and NGC6369 and in both cases the central star luminosity determined by our method was higher than the literature value. This is because it was assumed that these nebulae are radiation bound but we have shown them to be matter bound as they lose up to 70% of their ultraviolet (UV) radiation to space, resulting in an underestimation of both the luminosity and temperature. The blue rise in the SED for NGC6781 also confirms that blue radiation is escaping from the nebula. Note that the central star luminosity from our model, L = 385/$L^{\odot}$ is larger than the luminosity derived from the observed SED L = 225/$L^{\odot}$ by a factor of 1.7, confirming that the nebula is matter bound and that a significant fraction of the stellar UV flux escapes from the object.

We claim that ours are the most accurate luminosities and temperatures that have been determined for these stars to date. Interestingly our values tend to bring the core masses closer to 0.6 $M^{\odot}$which is also the peak value of the narrow mass distribution of white dwarfs.

We acknowledge the continuing support of National Optical Astronomy Observatory (NOAO)'s Science Fund to Hektor Monteiro and the generous hospitality of the Nordic Optical Telescope on La Palma.

Notes

1 Texto baseado em artigo de Schwarz e Monteiro (2006), publicado anteriormente em *The Astrophysical Journal*.

2 See <http://www.ing.iac.es/rcorradi>.

References

ACKER, A. et al. Strabourg-ESO catalogue of galactic planetary nebulae. *VizieR*, v. 84, 1992.

ALLER, L. H. *Physics of thermal gaseous nebulae*. 1. ed. Dordrecht: Reidel, 1894.

BLOCKER, T. Stellar evolution of low- and intermediate-mass stars II. Post-AGB evolution. *Astronomy & Astrophysics*, v. 299, p. 755-769, 1995.

CIARDULLO, R. Extragalactic Distances from Planetary Nebulae. *Lecture Notes in Physics*, v. 635, p.243-263, 2003.

CORRADI, R. L. M. et al. Ionized haloes in planetary nebulae: new discoveries, literature compilation and basic statistical properties. *Monthly Notices of the Royal Astronomical Society*, v. 340, n. 2, p. 417-446, 2003.

CORRADI, R. L. M.; SCHWARZ, H. E. Morphological populations of planetary nebulae: which progenitors? I. Comparative properties of bipolar nebulae. *Astronomy & Astrophysics*, v. 293, p. 871-888, 1995.

ERCOLANO, B. et al. Mocassin: a fully three-dimensional Monte Carlo photoionization code. *Monthly Notices of the Royal Astronomical Society*, v. 340, n. 4, p. 1136-1152, 2003.

FELDMEIER, J. J. et al. Intracluster planetary nebulae in the Virgo Cluster. III. Luminosity of the intracluster light and tests of the spatial distribution. *The Astrophysical Journal*, v. 615, n. 1, 196-208, 2004.

GURZADYAN, G. A. *The physics and dynamics of Planetary Nebulae*. 1. ed. New York: Springer, 1997.

IBEN JUNIOR, I.; RENZINI, A. Asymptotic giant branch evolution and beyond. *Annual Review of Astronomy and Astrophysics*, v. 21, p. 271-342, 1983.

IDIART, T. P.; COSTA, R. D. D.; MACIEL, W. J. Chemical evolution of the SMC: the planetary nebulae. In: INTERNATIONAL ASTRONOMICAL UNION SYMPOSIUM, 2003, Canberra. *Proceedings*... Canberra: IAU, 2003. v. 209. p. 581-581.

JACOBY, G. H.; CIARDULLO, R.; FELDMEIER, J. J. Future Directions for the Planetary Nebul Luminosity Function. In: EGRET, D.; HECK, A. *Harmonizing cosmic distance scales in a post-Hipparcos era*. 1. ed. San Francisco: Astronomical Society of the Pacific, 1999. ASP conference series, v. 167, p. 175-191.

KALER, J. B.; JACOBY, G. H. Central star temperatures of optically thick planetary nebulae and a distance-independent test of dredge-up theory. *The Astrophysical Journal*, v. 345, p. 871-880, 1989.

KALER, J.B., SHAW, R.A., BROWNING, L. An Electronic Emission-Line Catalog for Planetary Nebulae. *Publications of the Astronomical Society of the Pacific*, v. 109, p. 289-291, 1997.

LIU, Y. et al. Chemical abundances of planetary nebulae from optical recombination lines: I. Observations and plasma diagnostics. *Monthly Notices of the Royal Astronomical Society*, v. 353, n. 4, p. 1231-1250, 2004.

MAVROMATAKIS, F., PAPAMASTORAKIS, J.; PALEOLOGOU, E. V. The physical structure of the planetary nebula NGC 6781. *Astronomy & Astrophysics*, v. 374, p. 280-287, 2001.

MONTEIRO, H. et al. Morphology and kinematics of planetary nebulae. II. A diabolo model for NGC 3132. *The Astrophysical Journal*, v. 537, p. 853-860, 2000.

MONTEIRO, H. et al. Three-dimensional photoionization structure and distances of planetary nebulae I. NGC 6369. *The Astrophysical Journal*, v. 609, p. 194-202, 2004.

MONTEIRO, H. et al. Three-dimensional photoionization structure and distances of planetary nebulae II. Menzel 1. *The Astrophysical Journal*, v. 620, p. 321-329, 2005.

MYERS, P. C. et al. Near-infrared and optical observations of IRAS sources in and near dense cores. *The Astrophysical Journal*, v. 319, p. 340-357, 1987.

PHILLIPS, J. P. The relation between Zanstra temperature and morphology in planetary nebulae. *Monthly Notices of the Royal Astronomical Society*, v. 344, n. 2, 501-520, 2003.

POTTASCH, S. R. *Planetary nebulae: a study of late stages of stellar evolution*. 1. ed. Dordrecht: Reidel, 1984.

RICE, M., SCHWARZ, H. E., MONTEIRO, H. 3-D Structure and Distance of the Planetary Nebula Hb5. In: AMERICAN ASTRONOMICAL SOCIETY MEETING, 205., 2004, San Diego. *Bulletin*... San Diego: ASS, 2004. v. 36, p. 1.572.

SCHWARZ, H. E.; MONTEIRO, H. 3-D photoionization structure and distances of planetary. *The Astrophysical Journal*, v. 648, n. 1, p. 430-434, 2006.

STANGHELLINI, L. et al. The Correlations between Planetary Nebula Morphology and Central Star Evolution: Analysis of the Northern Galactic Sample. *The Astrophysical Journal*, v. 576, p. 285-293, 2002.

STANGHELLINI, L.; CORRADI, R. L. M.; SCHWARZ, H. E. The correlations between planetary nebula morphology and central star evolution. *Astronomy & Astrophysics*, v. 279, n. 2, p. 521-528, 1993.

VASSILIADIS, E.; WOOD, P. R. Post-asymptotic giant branch evolution of low- to intermediate-mass stars. *Astronomy and Astrophysics Supplement Series*, v. 92, p. 125-144, 1994.

Recebido em 18 set. 2006 / aprovado em 20 nov. 2006

Para referenciar este texto

SCHWARZ, H. E.; MONTEIRO, H. 3D photoionization structure and distances of Planetary Nebulae III. NGC 6781. *Exacta*, São Paulo, v. 4, n. 2, p. 281-288, jul./dez. 2006.